Inferring phenotypic plasticity and local adaptation to climate across tree species ranges using forest inventory data

Running title: Understanding phenotypic variation in natural populations

Thibaut Fréjaville[1*], Bruno Fady[2], Antoine Kremer[3], Alexis Ducousso[3], Marta Benito Garzón[1]

[1] *BIOGECO (UMR 1202), INRA, Univ Bordeaux, 33615 Pessac, France*

[2] *INRA, UR629, Ecologie des Forêts Méditerranéennes (URFM), 84914 Avignon, France*

[3] *BIOGECO (UMR 1202), INRA, Univ Bordeaux, 33610 Cestas, France*

[*] *Correspondence author. E-mail: thibaut.frejaville@gmail.com*

Acknowledgements

This study was funded by the "Investments for the Future" program IdEx Bordeaux (ANR-10-IDEX-03-02) and the European Union's Horizon 2020 research and innovation programme project GenTree (grant agreement No 676876). We are very grateful to Juan Fernandez Manjarrés (CNRS-Université Paris-Sud) with whom the discussion about how to use NFI for splitting genetic and plastic effects started many years ago. We are indebted to Denis Vauthier and Franck Rei (INRA UEFM, Avignon), Fabrice Bonne, Thierry Paul and Vincent Rousselet (INRA UEFL, Nancy) and Jean Gauvin (INRA UGBFOR, Orléans) for data collection in the *Abies alba* provenance tests. We acknowledge colleagues from different European institutions for providing access and use of provenance data in *Quercus petraea*: Jon Kehlet Hansen, University of Copenhagen, for Denmark; Brigitte Musch and the staff of the French Office National des Forêts for France; Hans-Martin Rau, Jochen Kleinschmit, Josef Svolba of Niedersächsische Forstliche Versuchsanstalt, Abteilung Forstpflanzenzüchtung, Staufenberg, Escherode and Wilfried Steiner, Alwin Janssen, Nordwestdeutsche Forstliche Versuchsanstalt, Abteilung Waldgenressourcen, Hann-Münden, for Germany; Władysław Chałupka, Henryk Fober of the Instytut Dendrologii PAN, Kórnik

29 for Poland; Steve J Lee, Alan M. Fletcher and Edward P. Cundall, Northern Research
30 Station, for the United Kingdom.

ABSTRACT

Aim: To test whether adaptive and plastic trait responses to climate across species distribution ranges can be untangled using field observations, under the rationale that, in natural forest tree populations, long-term climate shapes local adaptation while recent climate change drives phenotypic plasticity.

Location: Europe.

Time period: 1901-2014.

Taxa: Silver fir (*Abies alba* Mill.) and sessile oak (*Quercus petraea* (Matt.) Liebl.).

Methods: We estimated the variation of individual tree height as a function of long-term and short-term climates to tease apart local adaptation, plasticity and their interaction, using mixed-effect models calibrated with National Forest Inventory data (*in-situ* models). To validate our approach, we tested the ability of *in-situ* models to predict independently tree height observations in common gardens where local adaptation to climate of populations and their plasticity can be measured and separated. *In-situ* model predictions of tree height variation among provenances (populations of different geographical origin) and among planting sites were compared to observations in common gardens and to predictions from a similar model calibrated using common garden data (*ex-situ* model).

Results: In *Q. petraea*, we found high correlations between *in-situ* and *ex-situ* model predictions of provenance and plasticity effects and their interaction on tree height ($r > 0.80$). We showed that the *in-situ* models significantly predicted tree height variation among provenances and sites for *Abies alba* and *Quercus petraea*. Spatial predictions of phenotypic plasticity across species distribution ranges indicate decreasing tree height in populations of warmer climates in response to recent anthropogenic climate warming.

Main conclusions: Our modelling approach using National Forest Inventory observations provides a new perspective for understanding patterns of intraspecific trait variation across species ranges. Its application is particularly interesting for species for which common garden experiments do not exist or do not cover the entire climatic range of the species.

Keywords: *Abies alba*, common gardens, intraspecific trait variation, national forest inventory, *Quercus petraea*, tree height

INTRODUCTION

Understanding the causes of phenotypic variation across species distribution ranges is important because phenotypic traits are fundamental drivers of community assembly, ecosystem functioning, and population response to climate change (Diaz *et al.*, 2004; Shipley *et al.*, 2006; Alberto *et al.*, 2013; Kunstler *et al.*, 2016). The two non-exclusive causes of phenotypic variation within species are the phenotypic plasticity (i.e., the capacity of one genotype to render different phenotypes under different environments, Valladares *et al.*, 2006) and local adaptation (i.e., the fact that individuals have a better fitness in their local environment than individuals from other populations, Kawecki & Ebert, 2004). The spatial distribution of the amount of phenotypic variation that can be attributed to phenotypic plasticity or to local adaptation may change the response of organisms to climate change as predicted by theoretical approaches (Chevin *et al.*, 2010; Valladares *et al.*, 2014). Yet, attributing the cause of phenotypic trait variation across species ranges to either plastic or genetic components, or the interaction between the two, remains a challenge without using costly, long-term common garden experiments.

Long-term spatial divergence under different environmental conditions is known to promote phenotypic differentiation of populations as a result of local adaptation (Mimura &

78 Aitken, 2010; Savolainen *et al.*, 2013; Yeaman *et al.*, 2016), which affects their current
79 response to a particular climate (Rehfeldt *et al.*, 2002; Savolainen *et al.*, 2007; Valladares *et*
80 *al.*, 2014). However, significantly less is known about the distribution of phenotypic
81 plasticity and its importance for populations for coping with rapid climate change across the
82 species range, especially in long-lived sessile organisms such as forest trees (Nicotra *et al.*,
83 2010; Benito Garzón *et al.*, 2011; Valladares *et al.*, 2014; Duputié *et al.*, 2015).
84 Patterns of phenotypic plasticity and local adaptation of populations have long been
85 assessed using common garden or reciprocal transplant experiments, in which genotypes of
86 known climatic origin (i.e., provenances) are growing in experimental plantations where
87 short-term environmental conditions are controlled. In common gardens (also named
88 'provenance tests' or 'genetic trials'), local adaptation has mostly been inferred from trait
89 differences among provenances that are related to the long-term climate of origin of the
90 provenance, while plasticity is quantified by trait variation with the short-term climatic
91 conditions at the planting sites (see Matyas, 1994; Wang *et al.*, 2006; Leites *et al.*, 2012 for
92 forest trees). Common gardens have been established for a few economically important tree
93 species for which only a restricted range of populations and ontogenic stages have been
94 studied, which makes the understanding of phenotypic variation across species ranges limited
95 (Fady *et al.*, 2016).
96 On the other hand, causes of phenotypic variation are confounded in natural conditions, in
97 addition to the effects of ontogeny and competition. National Forest Inventories (NFI)
98 provide extensive data of phenotypic variation of forest trees in natural conditions, and hence,
99 they have been widely used to test different ecological questions such as the effects of
100 functional traits on competition, forest productivity and response to climate change (Kunstler

101 *et al.*, 2016; Ratcliffe *et al.*, 2016; Ruiz-Benito *et al.*, 2017), but to date, the causes of
102 phenotypic variation in NFI remain unexplored.

103 Here we show that the components of intraspecific trait variation: local adaptation,
104 plasticity and their interaction, can be statistically estimated using the field data recorded in
105 French NFI for two ecologically and economically important forest tree species usually
106 managed using natural regeneration, *Abies alba* Mill. and *Quercus petraea* (Matt.) Liebl. We
107 use tree height, an important adaptive and fitness-related trait (Savolainen *et al.*, 2007; Díaz
108 *et al.*, 2016), to independently test our approach on field observations (NFI) and we validate
109 our findings using common garden data. Our approach expands the space-for-time
110 substitution analysis developed in common gardens (Matyas, 1994; Rehfeldt *et al.*, 2002;
111 Leites *et al.*, 2012) to field observations of phenotypic trait variation, with the rationale that
112 trees inventoried in the field have a local origin (i.e. seed sources originated within the
113 bioclimatic region inhabited by the trees). To separate the sources of phenotypic variation in
114 nature, we examined climatic variations that occur at two temporal and spatial scales: first,
115 regional patterns in long-term climate (LTC) that have promoted trait variation among
116 provenances as a result of local adaptation (Savolainen *et al.*, 2007; Mimura & Aitken, 2010;
117 Kremer *et al.*, 2012); and, second, short-term climate (STC) that shapes plastic responses of
118 individual trees to recent climate change (Nicotra *et al.*, 2010; Valladares *et al.*, 2014). Our
119 approach opens new perspectives for the understanding of phenotypic variation patterns
120 across species distribution ranges using large field observation datasets such as forest
121 inventories.
122

METHODS

We analysed tree height (m), a fitness-related phenotypic trait, measured both in NFI and common gardens. We selected two major European forest species with contrasted life history traits and ecological requirements: *Abies alba* Mill. (a montane evergreen needle-leaved gymnosperm) and *Quercus petraea* (Matt.) Liebl. (a temperate deciduous broadleaved angiosperm). In the NFI, these two species are traditionally managed using natural regeneration, thus adult trees are assumed to derive from the local gene pool.

We calibrated two independent mixed-effect models of individual tree height using NFI (*in-situ* model) and common garden data (*ex-situ* model), respectively. To validate our models we used two different methods (Fig. 1). The first one is a validation using common garden data: it directly compares the results of the *in-situ* model with independent tree height measurements standardized by common garden and by provenance to respectively separate the effects of the provenance (local adaptation) and plasticity. The second one is a validation using *ex-situ* model predictions: it compares the predictions of *in situ* and *ex-situ* models regarding the relative contribution to the model of the climate of the planting site (plastic effect) and that of the climate of the origin of the provenances (local adaptation), and the interaction between both. All analyses and computations were carried out in the R software environment (R Core Team, 2013).

Phenotypic data

National Forest Inventories (NFI)

Observation data comprised ten annual campaigns of the French NFI (2005–2014; http://inventaire-forestier.ign.fr), which consists of a regular grid (1 km^2) of temporary forest plots of 707 m^2 each. In this study, we focused on French NFI (Appendix S1, Fig. S1.1)

147 because inventories of neighbouring countries do not provide age data, thereby preventing the
148 effect of age to be accounted for in models. Nevertheless, the distribution of French NFI plots
149 has a good representativeness of the climatic range of the two species (Fig. S2.1). In each
150 NFI plot, we selected trees for which height (in m), diameter at breast height (dbh; in cm) and
151 age (years) data were measured. In particular, tree age was estimated from wood increment
152 cores collected at breast height (1.30 m) for the one or two of the largest dominant trees in the
153 plot. To account for stand density and the local abundance of neighbouring trees on tree
154 height variation among plots, we computed for each NFI plot the sum of the basal area of
155 neighbouring trees larger than 7.5 cm dbh (Kunstler *et al.*, 2016). We removed plots outside
156 the natural distribution range of the species (Fig. S1.1), identified as plantation or if there was
157 any evidence of recent (<5 years) management, for example logging. We assumed that trees
158 in the remaining plots originated from local provenances within the same bioclimatic region.
159 The final dataset consisted of 5376 trees from 3614 plots for *Q. petraea*, and 1304 trees from
160 904 plots for *A. alba*.
161
162 *Common gardens*
163 Common garden data were used to independently validate *in-situ* models (NFI calibration).
164 They were established for breeding purposes during 1990–1996 for *Q. petraea* and 1967–
165 1972 for *A. alba*, as follows: (i) seeds were collected from seed sources (hereafter
166 provenances) throughout the natural distribution range of the species (N = 141 for *Q. petraea*,
167 N = 47 for *A. alba*); (ii) the seeds were sown in a nursery; (iii) seedlings were transplanted to
168 several sites, i.e., common gardens (N = 13 for *Q. petraea*, N = 6 for *A. alba*; Fig. S1.1),
169 using a randomised block design; and (iv) measurements of tree height were made at several
170 different years. To avoid pseudo-replication, we randomly selected a single measurement year

171 for each tree. Neighbour basal area was assumed to be constant because plantations have a
172 regular spacing design. Tree age at the time of height measurement was considered to be the
173 time since sowing. A detailed description of the *Q. petraea* provenance tests is provided in a
174 previous study (Sáenz-Romero *et al.*, 2017). A description of the *A. alba* provenances studied
175 in common gardens is provided in Appendix S1 (Tables S1-S2).
176
177 **Climate data**
178 To analyse phenotypic trait response to long-term climate and recent climate change, we used
179 the yearly climate grids (1901–2014) at 30 arc sec resolution (~1 km^2) of the EuMedClim
180 dataset covering Europe and the Mediterranean Basin (Fréjaville & Benito Garzón, 2018).
181 For the present study, the following bioclimatic variables were considered (Fig. S2.1): annual
182 mean temperature, maximum temperature of the warmest month, minimum temperature of
183 the coldest month, annual precipitation, precipitation of the wettest and the driest month,
184 annual potential evapotranspiration, potential evapotranspiration of the warmest and the
185 coldest month and water balance (precipitation minus potential evapotranspiration) of the
186 wettest and the driest month. EuMedClim was computed following an anomaly approach
187 using the fine 30' resolution of WorldClim climate means (version 1.4, Hijmans *et al.*, 2005)
188 to adjust the coarse spatial 0.5° resolution of yearly climate data from the Climate Research
189 Unit (version ts3.23, Harris *et al.*, 2014). EuMedClim provides inter-annual variation of
190 bioclimatic conditions at high spatial resolution, allowing the analysis of climate at different
191 spatial and temporal scales instead of using climate means over a reference period (e.g.
192 WorldClim).
193 To fulfil the requirements of our modelling approach based on the different climate scales
194 at which phenotypic plasticity and local adaptation act, we split the climate data into three

different sets of data: (i) long-term climate (LTC) that is the average climate value of the 1901–1960 period, and represents the climate driven local adaptation in the past for provenances (for common gardens) or for a common bioclimatic origin (for NFI, assuming that that all trees have a local origin in a given bioclimatic origin – Appendix S2); (ii) short-term climate (STC) represents the plastic response of trees to recent climate and is calculated as the local climate averaged over the 10 years preceding the measurements (NFI and common garden data); iii) recent climate change (RCC), calculated by subtracting LTC from STC to avoid collinearity problems between LTC and STC in NFI.

Models of intra-specific trait variability

Hereafter, we refer to models calibrated using NFI data as *in-situ* models and to models calibrated using common gardens as *ex-situ* models. For a given species, the phenotypic trait T_{ijk} (tree height) of the i^{th} tree individual of the j^{th} bioclimatic region (or provenance) in the k^{th} plot (or common garden) was modelled as follows:

$$\log(T_{ijk}) = \alpha_0 + \alpha_1 LTC_j + \alpha_2 LTC_j^2 + \alpha_3 RCC_{jk} + \alpha_4 RCC_{jk}^2 + \alpha_5 LTC_j \times RCC_{jk} + \beta + \delta + \varepsilon \quad (1)$$

where LTC_j is the long-term climate of either the j^{th} bioclimatic region in NFI or the j^{th} provenance in common gardens; RCC_{jk} is the recent climate change defined as the difference between the STC at the k^{th} site (i.e., the NFI plot or the common garden) and LTC_j. We included quadratic terms for both LTC_j and RCC_{jk} to consider linear and hump-shaped height responses to climate across species ranges. β includes ontogeny and neighbour basal area covariates and is defined as:

$$\beta = \alpha_6 \log(age_{ijk}) + \alpha_7 \log(BAc_{ijk}) + \alpha_6 \log(age_{ijk}) \times RCC_{jk} + \alpha_7 \log(BAc_{ijk}) \times LTC_j \quad (2)$$

where *age* is the tree age (in years, estimated at breast height in NFI and as the time since sowing in common gardens) and *BAc* is the sum of the basal area of neighbouring trees (assumed to be constant in common gardens). δ gathers random effects and ε is the model error. To control for differences among sampling units in soil fertility, management (or disturbances) and environmental factors not accounted for by fixed effects, we set as random effects the plot nested within the bioclimatic region in *in-situ* models and the block nested within the site in *ex-situ* models (randomised block design). In the case of *A. alba*, the bioclimatic region random effect was not retained because it inflated p-values of LTC terms in the *in-situ* model (high redundancy). One main difference between NFI and common garden data is the age of trees (Fig. S4.1). We reduced this difference by excluding old trees (> 200 years) in NFI and saplings (< 10 years) in common gardens, and we added *age* as a covariate in the models to control for ontogeny. To control for potential differences in growth response to climate change among ontogenic stages, we added the interaction term $age_{ijk} \times RCC_{jk}$ in both models. We also introduced *BAc* as covariate to control for neighbour basal area (Fig. S4.1) and the interaction term $BAc_{ijk} \times LTC_j$ to control for potential differences in neighbour basal area effects among bioclimatic regions in *in-situ* models. A saturated model form including $BAc_{ijk} \times RCC_{jk}$ and $age_{ijk} \times LTC_j$ interaction terms was not retained as it decreased model parsimony and the significance of parameters of interest. Models were fitted using the R package nlme (Pinheiro *et al.*, 2015). Coefficients of determination were used to compute the percentage of explained variance by fixed effects alone ($R^2_{marginal}$) and both fixed and random effects ($R^2_{conditional}$) (Nakagawa & Schielzeth, 2013).

For each species, we selected one single explanatory bioclimatic variable to represent LTC and RCC, the same between the two datasets (to enable comparison). The variable selection process was as follows. First, we fitted one model per dataset for each bioclimatic variable

(Fig. S2.1) using eqns (1-2). Second, we removed models when parameter estimates for LTC and RCC were not significant at $P = 0.1$ or when positive quadratic relationships were fit ($\alpha_2 > 0$ or $\alpha_4 > 0$) to keep models with decreasing tree height towards one or both ends of the climatic gradient. Third, competitive models were compared using the Akaike information criterion (AIC), and the final model selection was based on the lowest AIC values for both *in-situ* and *ex-situ* models (to enable comparison).

Model predictions

Separating local adaptation, plasticity and their interaction

Model coefficients were used to separate components of phenotypic variation by substituting RCC to its climatic components ($RCC_{jk} = STC_k - LTC_j$) in eqn. (1):

$$\log(T_{ijk}) = \alpha_0 + (\alpha_1 - \alpha_3)\, LTC_j + (\alpha_2 + \alpha_4 - \alpha_5)\, LTC_j^2 + \alpha_3\, STC_k + \alpha_4\, STC_k^2 + (\alpha_5 - 2\alpha_4)\, LTC_j \times RCC_{jk} + \beta + \delta + \varepsilon \qquad (3)$$

This analytical decomposition enables to estimate the relative effects of the long-term and short-term climate in the field, using RCC and LTC from eqn. (1). From eqn. (3), coefficients associated to linear ($\alpha_1 - \alpha_3$) and quadratic ($\alpha_2 + \alpha_4 - \alpha_5$) variation of LTC are used to predict the effect of the provenance (local adaptation), coefficients associated to linear (α_3) and quadratic (α_4) variation of STC are used to predict phenotypic plasticity (reaction norms) and those associated to $LTC_j \times STC_k$ ($\alpha_5 - 2\alpha_4$) are used to predict their interaction.

Spatial predictions

The *in-situ* and *ex-situ* models were used to make spatial predictions of provenance and plasticity effects, their interaction and the total component of tree height response to climate

265 across Europe. We computed LTC_j and STC_k in each grid cell (30 arc sec resolution)
266 respectively using the long-term (1901–1960) and the recent short-term (2001–2014)
267 averaged values of the corresponding climatic variables to compute maps according to fitted
268 parameters in eqn. (3). Effects of covariates were fixed for *age* (12-year-old trees), *BAc* (30
269 m^2 ha^{-1}) and for their interaction with RCC_{jk} and LTC_j (both averaged across the species
270 natural range), respectively, according to eqn. (2), and these constants (including the intercept
271 α_0) were added to the total variation component.

272

273 **Model validation**

274 To validate our approach, we used two alternative methods (Fig. 1) to test the ability of *in-*
275 *situ* models to predict independent tree height observations in common gardens where the
276 effects of the provenance, plasticity and their interaction can be separated.

277

278 *Validation using common garden data*

279 To compare the predictions of *in-situ* models with raw common garden data, we first
280 predicted the mean height of each provenance in each site (provenance-by-site mean) from
281 eqn. (3), as a function of the LTC of the provenance and the STC of the site for a given age
282 and neighbour basal area. Then, we compared these predictions to observed values in
283 common gardens. Both predicted and observed provenance-by-site means were standardized
284 across sites and provenances to estimate provenance and plasticity effects, respectively (see
285 Appendix S3). Correlations between predicted and observed values were tested using Pearson
286 correlation coefficients.

287

Validation using ex-situ model predictions

To compare the predictions of *in-situ* and *ex-situ* models, we predicted provenance and plasticity effects, and their interaction, as a function of LTC and STC conditions in common gardens using both *in-situ* and *ex-situ* models (see Appendix S3). From eqn. (3), the mean tree height of a provenance planted in several common gardens was predicted for a given age and neighbour basal area as a function of the LTC of the provenance (genetic effect) and the mean tree height of each provenance was predicted as a function of the STC of the site (plasticity of the provenance). Correlations between paired predictions from *in-situ* and *ex-situ* models of provenance and plasticity effects, their interaction and the sum of all three components of tree height (total variation) were tested using Pearson correlation coefficients. For the interaction component, correlation coefficients were computed separately for the mean plastic responses (reaction norms) of cold, core and warm provenances. We classified provenances among cold, core and warm parts of the range using the 1-33th, 34-66th and 67-100th percentiles of LTC, respectively, computed across the natural distribution range of the species.

RESULTS

We found both *in-situ* and *ex-situ* models with significant terms for LTC, RCC and their interaction on individual tree height in *Q. petraea* whereas only the *in-situ* model was found significant for *A. alba*. In *Q. petraea*, selected *in-situ* and *ex-situ* models were based on the maximum temperature of the warmest month (Tmax). In *A. alba*, the selected *in-situ* model was based on the potential evapotranspiration of the warmest month (PETmax). Both *in-situ* and *ex-situ* models indicated significant negative interaction between LTC and RCC (Table 1)

and positive interaction between LTC and STC (Table 2) in both species. Hence, average plasticity differed among regions and provenances for both species.

In-situ selected models indicated significant positive effects of tree age and neighbour basal area on tree height (Table 1, Fig. S4.1). Tree height increased with increasing neighbour basal area in *A. alba* ($P = 0.07$) and with neighbour basal area towards warmer regions in *Q. petraea* (positive interaction between BAc and LTC, $P = 0.02$; Table 1).

Statistical approximation of provenance and plasticity effects

Sessile oak (Quercus petraea)

Validation using common garden data indicated that predictions of tree height variation among provenances and among sites using the *in-situ* model were significantly correlated with observations in common gardens in *Q. petraea* ($P < 0.001$ for estimates of provenance and plasticity effects, and the total component of tree height, Fig. S6.3). Validation using *ex-situ* model predictions showed high correlations between *in-situ* and *ex-situ* model predictions of the provenance and plasticity effects, and their interaction (Table 2, Fig. 2). We found significant quadratic responses of height to Tmax for the provenance effect (Fig. 2a), plasticity (Fig. 2b) and the total (Fig. 2c) variation, that were similar between *in-situ* and *ex-situ* models with high correlations between paired predictions ($r > 0.80$, $P < 0.001$). We found high correlations between *ex-situ* and *in-situ* model paired predictions of cold ($r = 0.65$, $P < 0.001$), core ($r = 0.99$, $P < 0.001$) and warm provenance mean reaction norms ($r = 0.97$, $P < 0.001$). Both models showed similar patterns in Tmax optimums (i.e. Tmax values corresponding to maximum predicted heights) among cold, core and warm provenances that were respectively warmer and colder for warm and cold provenances (Kruskal-Wallis tests, *P*

334 < 0.001, Fig. 2d-e). The *in-situ* model, however, showed higher differences in optimums
335 among provenances (Fig. 2e).
336
337 *Silver fir (Abies alba)*
338 In *A. alba*, the *in-situ* model showed significant quadratic responses of tree height to PETmax
339 for the provenance and plasticity effects (Table 2). Validation using common garden data
340 indicated that the *in-situ* model significantly predicted tree height variation among
341 provenances in common gardens (provenance effect: $r = 0.44$, $P < 0.01$, Fig. 3a) and among
342 sites (plasticity effect: $r = 0.72$, $P < 0.001$, Fig. 3b). The correlation was weak for the total
343 variation ($r = 0.20$, $P = 0.06$, Fig. 3c, Fig. S7.3). The *in-situ* model predicted warmer
344 optimums for warm provenances and colder optimums for cold provenances (Kruskal-Wallis
345 tests, $P < 0.001$, Fig. 3d).
346
347 **Range-wide spatial predictions of tree height**
348 In *Q. petraea*, both the *ex-situ* and *in-situ* models predicted very similar spatial patterns (Fig.
349 4) in the relative variation of tree height for provenance and plasticity effects, and their
350 interaction, despite differences in absolute values for total variation for a given age and
351 neighbour basal area (Fig. 4g-h). These differences are explained by the differences in tree
352 age estimation between the two datasets (i.e. age is measured at breast height in NFI and as
353 the time since sowing in common gardens). The quadratic response of tree height to LTC
354 (Fig. 2a) predicted that trees living at the warm limit of the species range were the shortest,
355 which is illustrated by the short heights predicted over southern Europe from the provenance
356 effect (transparent colours, Fig. 4a-b). Similarly, trees inhabiting the warmest conditions in
357 the southernmost part of the species distribution range were also predicted to be shorter from

the phenotypic plasticity effect (Fig. 4c-d). Spatial predictions of interaction effects showed an opposite pattern with increasing height towards warmer climates (Fig. 4e-f). Total variation followed spatial patterns of the provenance and plasticity effects (Fig. 4g-h). In *A. alba*, trees inhabiting cold climates (e.g. high elevation areas in the Alps) were predicted to be shorter according to the *in-situ* model (Fig. 5). In warm climates, the provenance effect (Fig. 4a) and provenance × plasticity interaction (Fig. 5c) predicted taller trees while plasticity predicted smaller trees over southern Europe (Fig. 5b).

DISCUSSION

Can local adaptation and phenotypic plasticity in tree height be inferred from *in-situ* observations?

To date, disentangling the sources of phenotypic variation has only been addressed by analysing common gardens or reciprocal transplant experiments (e.g. Kawecki & Ebert, 2004; Hoffmann & Sgrò, 2011; Blanquart *et al.*, 2013; Latreille & Pichot, 2017), using similar approaches as those that we named here *ex-situ* models. However, as common garden data are often scarce, we propose an alternative method for understanding the causes of phenotypic variation: using increasingly abundant data from field observations, such as NFI. Using the rationale of *ex-situ* models based on common garden data, we defined *in-situ* models based on NFI data and thoroughly validated *in-situ* model predictions with raw data coming from common gardens and with predictions from *ex-situ* models.

Overall, our results show that *in-situ* models correctly predicted phenotypic patterns observed in common gardens (Table 2, Figs 2-5), suggesting that field observations (NFI) can be used to statistically approximate the range-wide intraspecific variation in tree height that is attributable to local adaptation (provenance effects), plasticity and their interaction

components. In particular, our results suggest that differences among provenances that are related to their climate of origin can be statistically approximated using field measurements by modelling trait variation as a function of the long-term regional climate (LTC), while the recent climate change (RCC) and its components (STC - LTC) can be used to estimate the plastic response of the trait. However, we must keep in mind that other models can achieve similar predictions. Hence further studies are needed to decipher whether our approach can be used to estimate local adaptation and phenotypic plasticity components of intraspecific variation in the field for other traits and taxa.

In both species, the most parsimonious models (both *in-situ* and *ex-situ*) were based on climatic variables related to summer temperature: PETmax in *A. alba* and Tmax in *Q. petraea*. This underlies the high sensitivity of *Abies alba* to the evaporative demand in summer (Lebourgeois *et al.*, 2013) and that temperature chiefly drove differences in tree height among *Q. petraea* provenances while drought mostly drove plastic responses for tree height and survival in this species (Sáenz-Romero *et al.*, 2017).

Although validation analyses showed good agreement between *in-situ* model predictions and common garden data for both species, we found some discrepancies. In *A. alba*, we did not find any significant *ex-situ* model. This may be explained by the fact that less common garden data are available for this species compared to *Q. petraea*. In addition, *A. alba* is a generalist species with limited local adaptation to temperature and water availability (Frank *et al.*, 2017; Latreille & Pichot, 2017). Otherwise, predictions based on NFI data in *Q. petraea* (Fig. 2d) showed higher differences of climatic optima among provenances than those based on common garden data (Fig. 2e). These differences might be induced by intrinsic differences in the nature of data. The large difference in the age of trees (older in NFI data) and the fact that NFI data rely on dominant trees might partly explained these differences and the fact that

406 a stronger signal of local adaptation (i.e. higher differences in climatic optima) was found
407 using NFI data.
408
409 **Common patterns of local adaptation and plasticity in tree height: implications for**
410 **species distribution ranges under climate change**
411 In both species, we found hump-shaped relationships between height and climate for the
412 provenance (long-term climate) and plasticity effects (short-term climate) and a positive
413 interaction effect between them (Table 2, Figs 2-3). The latter indicated that climatic optima
414 of provenances co-vary positively with their climate of origin: warmer provenances grow
415 taller in warmer climates and colder provenances grow taller in colder climates (Figs 2d-e
416 and 3d). In addition, this indicated that plasticity differs significantly among populations, as
417 for other species (Wang *et al.*, 2006; Leites *et al.*, 2012; Münzbergová *et al.*, 2017; Sáenz-
418 Romero *et al.*, 2017). This consistency between *A. alba* (a mountain evergreen conifer tree)
419 and *Q. petraea* (a temperate deciduous broadleaved tree) points to potential common patterns
420 in local adaptation and plasticity among tree species, as recently indicated in boreal conifer
421 trees (Pedlar & McKenney, 2017).
422 Our spatial predictions of phenotypic plasticity suggest that tree height of warm
423 provenances has decreased in response to recent climate warming, mostly in southern Europe
424 (Figs 4-5). These results suggest that recent warming may have pushed species at the
425 warmest boundary of the distribution range beyond their tolerance limits, that is corroborated
426 by a higher mortality in warmest/driest range margins for *A. alba*, *Q. petraea* and other
427 European tree species (Cailleret *et al.*, 2014; Benito Garzón *et al.*, 2018). Furthermore, we
428 found that the effect of neighbour basal area on tree height was dependent on the climate of
429 the bioclimatic region in *Q. petraea*, emphasising that tree sensitivity to biotic interaction

(e.g. competition) may change along climatic gradients (Gomez-Aparicio *et al.*, 2011; Kunstler *et al.*, 2016).

CONCLUSION

We show that local adaptation and plasticity components of phenotypic variation, and their interaction, can be statistically approximated using field observations of wild tree populations subject to recent climate warming. However, further studies are needed to determine whether the ability of *in-situ* models to predict trends in common garden experiments represent a shared underlying cause that can be generalized to other situations, i.e. whether climate variations at different scales can be used to separate local adaptation and plastic responses to climate in field conditions. The modelling framework used in our study could be applied to many species and traits, offering a promising avenue to enhance our understanding of local adaptation and plasticity patterns across large geographical gradients.

REFERENCES

Alberto, F.J., Aitken, S.N., Alía, R., González-Martínez, S.C., Hänninen, H., Kremer, A., Lefèvre, F., Lenormand, T., Yeaman, S., Whetten, R. & Savolainen, O. (2013) Potential for evolutionary responses to climate change – evidence from tree populations. *Global Change Biology*, **19**, 1645–1661.

Benito Garzón, M., Alía, R., Robson, T.M. & Zavala, M.A. (2011) Intra-specific variability and plasticity influence potential tree species distributions under climate change. *Global Ecology and Biogeography*, **20**, 766–778.

Benito Garzón, M., González-Muñoz, N., Wigneron, J.-P., Moisy, C., Fernández-Manjarrés, J. & Delzon, S. (2018) The legacy of water deficit on populations having experienced negative hydraulic safety margin. *Global Ecology and Biogeography*, **in press**, 1–11.

Blanquart, F., Kaltz, O., Nuismer, S.L. & Gandon, S. (2013) A practical guide to measuring local adaptation. *Ecology Letters*, **16**, 1195–1205.

Cailleret, M., Nourtier, M., Amm, A., Durand-Gillmann, M. & Davi, H. (2014) Drought-induced decline and mortality of silver fir differ among three sites in Southern France. *Annals of Forest Science*, **71**, 643–657.

Chevin, L.-M., Lande, R. & Mace, G.M. (2010) Adaptation, Plasticity, and Extinction in a Changing Environment: Towards a Predictive Theory. *PLOS Biology*, **8**, e1000357.

Diaz, S., Hodgson, J.G., Thompson, K., Cabido, M., Cornelissen, J.H.C., Jalili, A., Montserrat-Marti, G., Grime, J.P., Zarrinkamar, F., Asri, Y. & others (2004) The plant traits that drive ecosystems: evidence from three continents. *Journal of vegetation science*, **15**, 295–304.

Díaz, S., Kattge, J., Cornelissen, J.H.C., Wright, I.J., Lavorel, S., Dray, S., Reu, B., Kleyer, M., Wirth, C., Colin Prentice, I., Garnier, E., Bönisch, G., Westoby, M., Poorter, H., Reich, P.B., Moles, A.T., Dickie, J., Gillison, A.N., Zanne, A.E., Chave, J., Joseph Wright, S., Sheremet'ev, S.N., Jactel, H., Baraloto, C., Cerabolini, B., Pierce, S., Shipley, B., Kirkup, D., Casanoves, F., Joswig, J.S., Günther, A., Falczuk, V., Rüger, N., Mahecha, M.D. & Gorné, L.D. (2016) The global spectrum of plant form and function. *Nature*, **529**, 167–171.

Duputié, A., Rutschmann, A., Ronce, O. & Chuine, I. (2015) Phenological plasticity will not help all species adapt to climate change. *Global Change Biology*, **21**, 3062–3073.

Fady, B., Cottrell, J., Ackzell, L., Alía, R., Muys, B., Prada, A. & González-Martínez, S.C. (2016) Forests and global change: what can genetics contribute to the major forest management and policy challenges of the twenty-first century? *Regional Environmental Change*, **16**, 927–939.

Frank, A., Howe, G.T., Sperisen, C., Brang, P., St Clair, J.B., Schmatz, D.R. & Heiri, C. (2017) Risk of genetic maladaptation due to climate change in three major European tree species. *Global Change Biology*.

Fréjaville, T. & Benito Garzón, M. (2018) The EuMedClim Database: Yearly Climate Data (1901–2014) of 1 km Resolution Grids for Europe and the Mediterranean Basin. *Frontiers in Ecology and Evolution*, **6**.

Gomez-Aparicio, L., Garcia-Valdes, R., Ruiz-Benito, P. & Zavala, M.A. (2011) Disentangling the relative importance of climate, size and competition on tree growth in Iberian forests: Implications for forest management under global change. *Global Change Biology*, **17**, 2400–2414.

Harris, I., Jones, P. d., Osborn, T. j. & Lister, D. h. (2014) Updated high-resolution grids of monthly climatic observations – the CRU TS3.10 Dataset. *International Journal of Climatology*, **34**, 623–642.

Hijmans, R.J., Cameron, S.E., Parra, J.L., Jones, P.G. & Jarvis, A. (2005) Very high resolution interpolated climate surfaces for global land areas. *International journal of climatology*, **25**, 1965–1978.

Hoffmann, A.A. & Sgrò, C.M. (2011) Climate change and evolutionary adaptation. *Nature*, **470**, 479–485.

Kawecki, T.J. & Ebert, D. (2004) Conceptual issues in local adaptation. *Ecology letters*, **7**, 1225–1241.

Kremer, A., Ronce, O., Robledo-Arnuncio, J.J., Guillaume, F., Bohrer, G., Nathan, R., Bridle, J.R., Gomulkiewicz, R., Klein, E.K., Ritland, K., Kuparinen, A., Gerber, S. & Schueler, S. (2012) Long-distance gene flow and adaptation of forest trees to rapid climate change. *Ecology Letters*, **15**, 378–392.

Kunstler, G., Falster, D., Coomes, D.A., Hui, F., Kooyman, R.M., Laughlin, D.C., Poorter, L., Vanderwel, M., Vieilledent, G., Wright, S.J. & others (2016) Plant functional traits have globally consistent effects on competition. *Nature*, **529**, 204–207.

Latreille, A.C. & Pichot, C. (2017) Local-scale diversity and adaptation along elevational gradients assessed by reciprocal transplant experiments: lack of local adaptation in silver fir populations. *Annals of Forest Science*, **74**, 77.

Lebourgeois, F., Gomez, N., Pinto, P. & Mérian, P. (2013) Mixed stands reduce Abies alba tree-ring sensitivity to summer drought in the Vosges mountains, western Europe. *Forest Ecology and management*, **303**, 61–71.

Leites, L.P., Robinson, A.P., Rehfeldt, G.E., Marshall, J.D. & Crookston, N.L. (2012) Height-growth response to climatic changes differs among populations of Douglas-fir: a novel analysis of historic data. *Ecological Applications*, **22**, 154–165.

Matyas, C. (1994) Modeling climate change effects with provenance test data. *Tree Physiology*, **14**, 797–804.

Mimura, M. & Aitken, S.N. (2010) Local adaptation at the range peripheries of Sitka spruce. *Journal of evolutionary biology*, **23**, 249–258.

Münzbergová, Z., Hadincová, V., Skálová, H. & Vandvik, V. (2017) Genetic differentiation and plasticity interact along temperature and precipitation gradients to determine plant performance under climate change. *Journal of Ecology*, **105**, 1358–1373.

Nakagawa, S. & Schielzeth, H. (2013) A general and simple method for obtaining R2 from generalized linear mixed-effects models. *Methods in Ecology and Evolution*, **4**, 133–142.

Nicotra, A.B., Atkin, O.K., Bonser, S.P., Davidson, A.M., Finnegan, E.J., Mathesius, U., Poot, P., Purugganan, M.D., Richards, C.L., Valladares, F. & van Kleunen, M. (2010) Plant phenotypic plasticity in a changing climate. *Trends in Plant Science*, **15**, 684–692.

Pedlar, J.H. & McKenney, D.W. (2017) Assessing the anticipated growth response of northern conifer populations to a warming climate. *Scientific Reports*, **7**.

Pinheiro, J., Bates, D., DebRoy, S., Sarkar, D. & R Core Team (2015) nlme: Linear and Nonlinear Mixed Effects Models. R package version 3.1–120. *http://CRAN.R-project.org/package=nlme*.

R Core Team (2013) *R: A language and environment for statistical computing*, R Foundation for Statistical Computing, Vienna, Austria.

Ratcliffe, S., Liebergesell, M., Ruiz-Benito, P., Madrigal Gonzalez, J., Muñoz Castañeda, J.M., Kändler, G., Lehtonen, A., Dahlgren, J., Kattge, J., Peñuelas, J. & others (2016) Modes of functional biodiversity control on tree productivity across the European continent. *Global ecology and biogeography*, **25**, 251–262.

Rehfeldt, G.E., Tchebakova, N.M., Parfenova, Y.I., Wykoff, W.R., Kuzmina, N.A. & Milyutin, L.I. (2002) Intraspecific responses to climate in Pinus sylvestris. *Global Change Biology*, **8**, 912–929.

Ruiz-Benito, P., Ratcliffe, S., Zavala, M.A., Martínez-Vilalta, J., Vilà-Cabrera, A., Lloret, F., Madrigal-González, J., Wirth, C., Greenwood, S., Kändler, G., Lehtonen, A., Kattge, J., Dahlgren, J. & Jump, A.S. (2017) Climate- and successional-related changes in functional composition of European forests are strongly driven by tree mortality. *Global Change Biology*, **23**, 4162–4176.

Sáenz-Romero, C., Lamy, J.-B., Ducousso, A., Musch, B., Ehrenmann, F., Delzon, S., Cavers, S., Chałupka, W., Dağdaş, S., Hansen, J.K., Lee, S.J., Liesebach, M., Rau, H.-M., Psomas, A., Schneck, V., Steiner, W., Zimmermann, N.E. & Kremer, A. (2017) Adaptive and plastic responses of Quercus petraea populations to climate across Europe. *Global Change Biology*, **23**, 2831–2847.

Savolainen, O., Lascoux, M. & Merilä, J. (2013) Ecological genomics of local adaptation. *Nature Reviews Genetics*, **14**, 807–820.

Savolainen, O., Pyhäjärvi, T. & Knürr, T. (2007) Gene flow and local adaptation in trees. *Annual Review of Ecology, Evolution, and Systematics*, 595–619.

Shipley, B., Vile, D. & Garnier, E. (2006) From plant traits to plant communities: a statistical mechanistic approach to biodiversity. *Science*, **314**, 812–814.

Valladares, F., Matesanz, S., Guilhaumon, F., Araújo, M.B., Balaguer, L., Benito-Garzón, M., Cornwell, W., Gianoli, E., Kleunen, M., Naya, D.E. & others (2014) The effects of phenotypic plasticity and local adaptation on forecasts of species range shifts under climate change. *Ecology letters*, **17**, 1351–1364.

Valladares, F., Sanchez-Gomez, D. & Zavala, M.A. (2006) Quantitative estimation of phenotypic plasticity: bridging the gap between the evolutionary concept and its ecological applications. *Journal of Ecology*, **94**, 1103–1116.

Wang, T., Hamann, A., Yanchuk, A., O'neill, G.A. & Aitken, S.N. (2006) Use of response functions in selecting lodgepole pine populations for future climates. *Global Change Biology*, **12**, 2404–2416.

Yeaman, S., Hodgins, K.A., Lotterhos, K.E., Suren, H., Nadeau, S., Degner, J.C., Nurkowski, K.A., Smets, P., Wang, T., Gray, L.K., Liepe, K.J., Hamann, A., Holliday, J.A., Whitlock, M.C., Rieseberg, L.H. & Aitken, S.N. (2016) Convergent local adaptation to climate in distantly related conifers. *Science*, **353**, 1431–1433.

DATA ACCESSIBILITY

Raw data can be freely accessed online for French National Forest Inventories (http://inventaire-forestier.ign.fr), *Quercus petraea* (https://arachne.pierroton.inra.fr/QuercusPortal/) and *Abies alba* common gardens (online repository, under process). Climate data used for this study are available online (http://gentree.data.inra.fr/climate/). R codes used for data analyses can be obtained from the correspondence author upon request.

BIOSKETCH

The authors' research aims to understand how ecological and evolutionary processes drive the effects of global changes on forests, by merging expertise in ecological modelling, genetics and conservation.

T.F. and M.B.G. conceived and designed the study; T.F. conducted the data analyses; T.F. and M.B.G. wrote the manuscript that was commented and improved by B.F., A.K. and A.D.

TABLES

Table 1 Estimates of *in-situ* and *ex-situ* linear mixed-effect models of individual tree height data (log-transformed). *In-situ* models were fit on 5376 trees (height measurements) in 3617 plots nested in 22 bioclimatic regions (random groups) for *Q. petraea* and on 1304 trees in 904 plots nested in 15 bioclimatic regions for *A. alba*. Bioclimatic regions were added as random effects in *in-situ* model for *Q. petraea* but not for *A. alba*. *Ex-situ* models were fit on 130241 trees (height measurements) from 141 provenances that were planted in 591 blocs nested in 13 sites (random groups) for *Q. petraea* and on 13314 trees from 47 provenances planted in 166 blocs nested in 6 sites for *A. alba*. No significant *ex-situ* models were found in *A. alba*. The climatic variable used to compute LTC and RCC is the maximal temperature of the warmest month in *Quercus petraea* and the potential evapotranspiration of the warmest month in *Abies alba*. The percentage of the variance explained by the models is measured by the marginal (fixed effects, m) and conditional (both fixed and random effects, c) adjusted R^2. 'Df' degree of freedom, 'BAc' sum of basal area of neighbouring competitor trees, 'LTC' long-term climate, 'RCC' recent climate change.

Table 2 Mean bootstrap estimates (± SD) of tree height variation due to provenance and plasticity effects, and their interaction, computed from *in-situ* (NFI) model and *ex-situ* (common garden) model. 'x' and 'x^2' indicate linear and quadratic terms respectively. Significant differences of bootstrapped values (n = 200) to null values were tested using t-tests; all are significant at $P < 0.001$.

481 **Table 1**

	in-situ				*ex-situ*			
Quercus petraea	**Estimate (±SE)**	**Df**	**t-value**	***P***	**Estimate (±SE)**	**Df**	**t-value**	***P***
Intercept	-13.40 (4.07)	3589	-3.3	0.001	-12.38 (2.23)	129643	-5.54	<0.001
log(age)	0.311 (0.009)	1758	34.53	<0.001	1.322 (0.008)	129643	167.71	<0.001
log(BAc)	-0.171 (0.133)	1758	-1.29	0.197				
LTC	1.269 (0.354)	19	3.59	0.002	0.903 (0.181)	129643	5	<0.001
LTC^2	-0.028 (0.008)	19	-3.58	0.002	-0.020 (0.004)	129643	-5.55	<0.001
RCC	0.440 (0.118)	3589	3.72	<0.001	0.730 (0.182)	129643	4.01	<0.001
RCC^2	-0.017 (0.003)	3589	-5.22	<0.001	-0.018 (0.004)	129643	-4.95	<0.001
LTC:RCC	-0.018 (0.005)	3589	-4.02	<0.001	-0.031 (0.007)	129643	-4.26	<0.001
log(BAc):LTC	0.013 (0.006)	1758	2.38	0.017				
log(age):RCC	0.009 (0.007)	1758	1.3	0.193	-0.012 (0.003)	129643	-3.63	<0.001
R2 (m/c) (%)	41/91				26/65			
Abies alba	**Estimate (±SE)**	**Df**	**t-value**	***P***				
Intercept	0.732 (0.649)	898	-1.13	0.259				
log(age)	0.319 (0.014)	396	23.57	<0.001				
log(BAc)	0.224 (0.123)	396	1.82	0.069				
LTC	0.024 (0.008)	898	2.95	0.003				
LTC^2	$-7.3\ 10^{-5}$ ($2.8\ 10^{-5}$)	898	-2.63	0.009				
RCC	0.009 (0.006)	898	1.46	0.146				
RCC^2	$-9.9\ 10^{-5}$ ($2.3\ 10^{-5}$)	898	-4.36	<0.001				
LTC:RCC	$-8.3\ 10^{-5}$ ($3.8\ 10^{-5}$)	898	-2.17	0.030				
log(BAc):LTC	$-2.4\ 10^{-4}$ ($9.5\ 10^{-4}$)	396	-0.25	0.803				
log(age):RCC	0.002 ($8.4\ 10^{-4}$)	396	1.92	0.056				
R2 (m/c) (%)	49/86							

482

483 **Table 2**

	Provenance effect		Phenotypic plasticity		interaction
	x	**x^2**	**x**	**x^2**	
***Quercus petraea* ex-situ model**	0.191 (0.026)	$-7.3\ 10^{-3}$ ($0.35\ 10^{-3}$)	0.712 (0.169)	-0.017 (0.003)	$4.6\ 10^{-3}$ ($0.68\ 10^{-3}$)
***Quercus petraea* in-situ model**	0.548 (0.365)	-0.022 (0.009)	0.465 (0.122)	-0.018 (0.003)	0.018 (0.007)
***Abies alba* in-situ model**	0.014 (0.007)	$-8.6\ 10^{-5}$ ($2.1\ 10^{-5}$)	0.010 (0.007)	$-9.2\ 10^{-5}$ ($2.1\ 10^{-5}$)	$1.0\ 10^{-4}$ ($0.4\ 10^{-4}$)

484

FIGURES

Figure 1 Workflow of the modelling approach and validation methods. We used individual tree height data from National Forest Inventories (NFI) to calibrate a mixed-effect model ('*in-situ* model') as a function of long-term climate (LTC) of the bioclimatic region and short-term climate (STC) of the forest plot to disentangle local adaptation, plasticity and their interaction on intraspecific trait variation. To validate our approach, we compared *in-situ* model predictions with independent observations of tree height variation in common gardens where trait differences among populations of different geographical origin (i.e., the provenance) and their plasticity can be separated. *In-situ* model predictions of tree height variation among provenances and among planting sites were compared to observations in common gardens (*validation using common garden data*) and to predictions from a parallel model calibrated using common garden data (*validation using ex-situ model predictions*). *Validation using ex-situ model predictions* needs common garden data covering large climatic gradients (as is the case of *Quercus petraea* in this study) which is not always feasible, while *validation using common garden data* can be used also with scarce common data networks (as is the case of *Abies alba* in this study).

Figure 2 Comparison of *in-situ* model (NFI) and *ex-situ* model (common gardens) predictions of provenance (a) and plasticity effects (b), and the total component (c) of tree height variation, recorded in common gardens in *Quercus petraea*. Pearson correlation coefficients between *ex-situ* and *in-situ* model predictions are reported. (d-e) Model predictions of plastic responses among provenances (provenance × plasticity interaction). Temperature optima for cold, core and warm provenances are indicated by horizontal boxplots; vertical coloured lines indicate mean optimum values. Significant differences in

509 temperature optimum were tested using Kruskal-Wallis tests: $\chi^2 = 105.2$ in d) and $\chi^2 = 104.2$
510 in e), $P < 0.001$ for both. Shaded areas and lines represent the standard deviation around
511 average model predictions (computed by bootstrapping in a-c). Predictions were scaled
512 between 0–1 independently for *in-situ* and *ex-situ* models. Model parameters (coefficients
513 and significance) are presented in Table 1. Validation analyses using common garden data are
514 presented in Appendix S3.
515
516 **Figure 3** Comparison of *in-situ* (NFI) model predictions and common garden data (*ex-situ*)
517 estimates of provenance (a) and plasticity effects (b), and the total component (c) of tree
518 height variation, recorded in common gardens in *Abies alba*. Points represent provenance
519 means in a) and provenance-by-site means in b-c that were computed according to the
520 validation method using common garden data (see Fig. 1). Computation of provenance and
521 plasticity effects, and the total variation is described in Appendix S3. Pearson correlation
522 coefficients between *ex-situ* data and *in-situ* model predictions are reported. (d) *In-situ* model
523 predictions of plastic responses among provenances (provenance × plasticity interaction).
524 Temperature optima for cold, core and warm provenances are indicated by horizontal
525 boxplots; vertical coloured lines indicate mean optimum values. Significant differences in
526 temperature optimum were tested using Kruskal-Wallis tests: $\chi^2 = 105.2$, $P < 0.001$. Shaded
527 areas and lines represent the standard deviation around average model predictions (computed
528 by bootstrapping in a-c). Height values were scaled between 0–1 independently for *in-situ*
529 predictions and common garden data. *In-situ* model parameters (coefficients and significance)
530 are presented in Table 1.
531

532 **Figure 4** Spatial predictions of *Quercus petraea* range-wide variation in tree height using *ex-*
533 *situ* (a, c, e, g) and *in-situ* models (b, d, f, h). Maps indicate the provenance effect (a-b),
534 plasticity (c-d), their interaction (e-f) and the total variation of tree height (g-h). The shaded
535 area represents model predictions outside the natural distribution range of the species.
536 Predictions are for 12-years-old trees, with neighbour basal area set to average conditions (30
537 m^2 ha^{-1}) in the *in-situ* model.
538
539 **Figure 5** Spatial predictions of *Abies alba* range-wide variation in tree height using the *in-*
540 *situ* model. Maps indicate the provenance effect (a), plasticity (b), their interaction (c) and the
541 total variation of tree height (d). The shaded area represents model predictions outside the
542 natural distribution range of the species. Predictions are for 12-years-old trees, with
543 neighbour basal area set to average conditions (30 m^2 ha^{-1}).

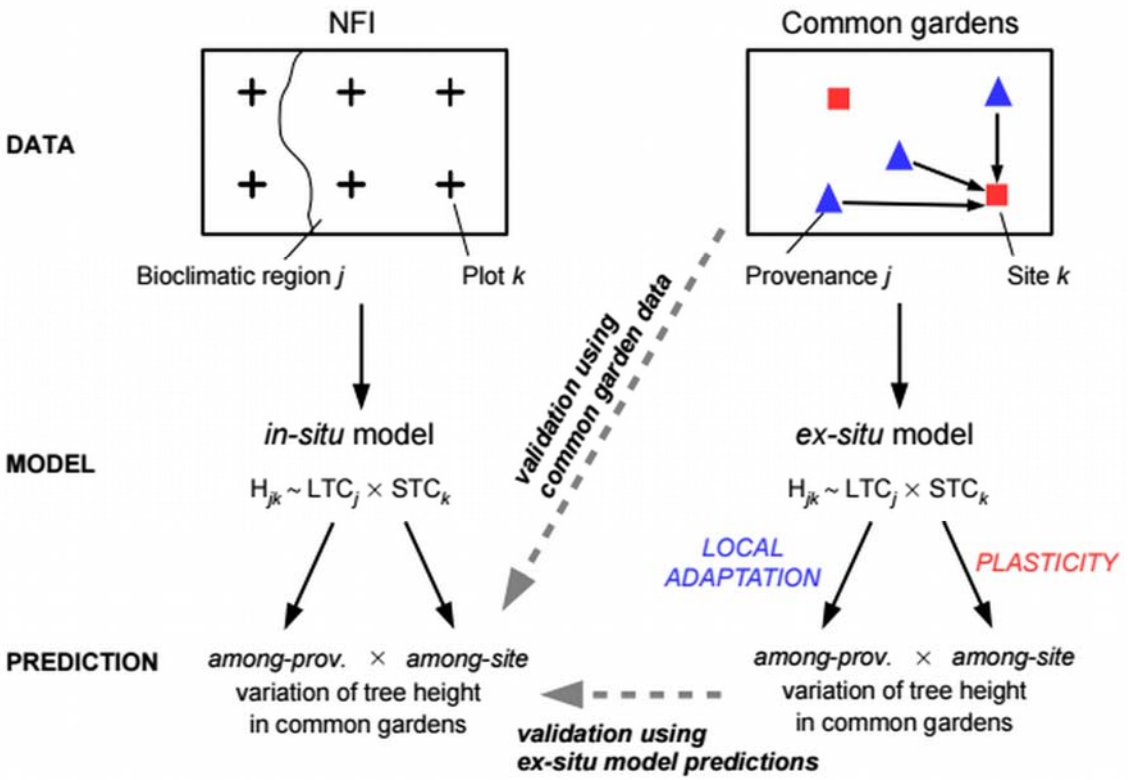

544

545 **Figure 1**

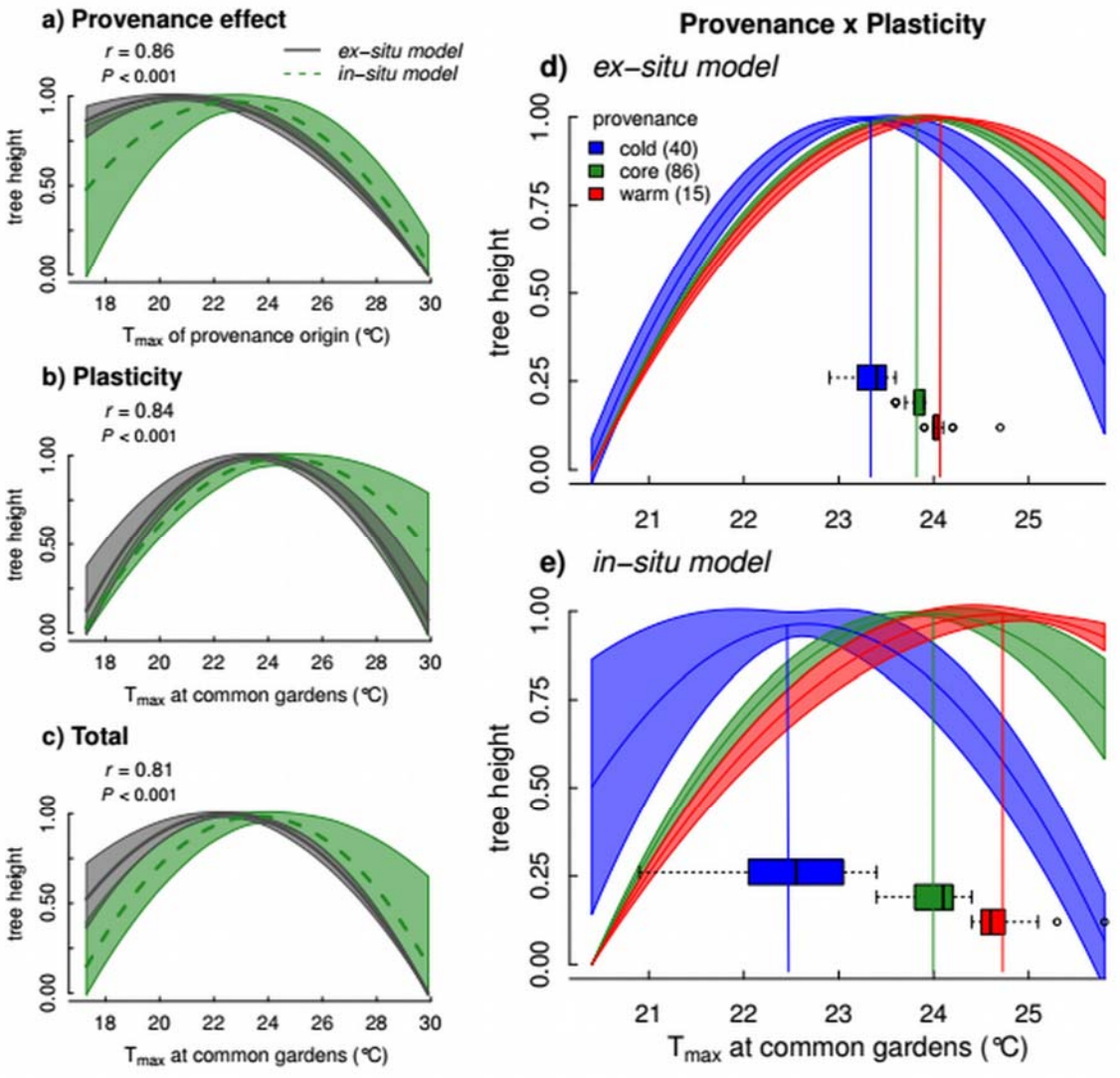

546

547 **Figure 2**

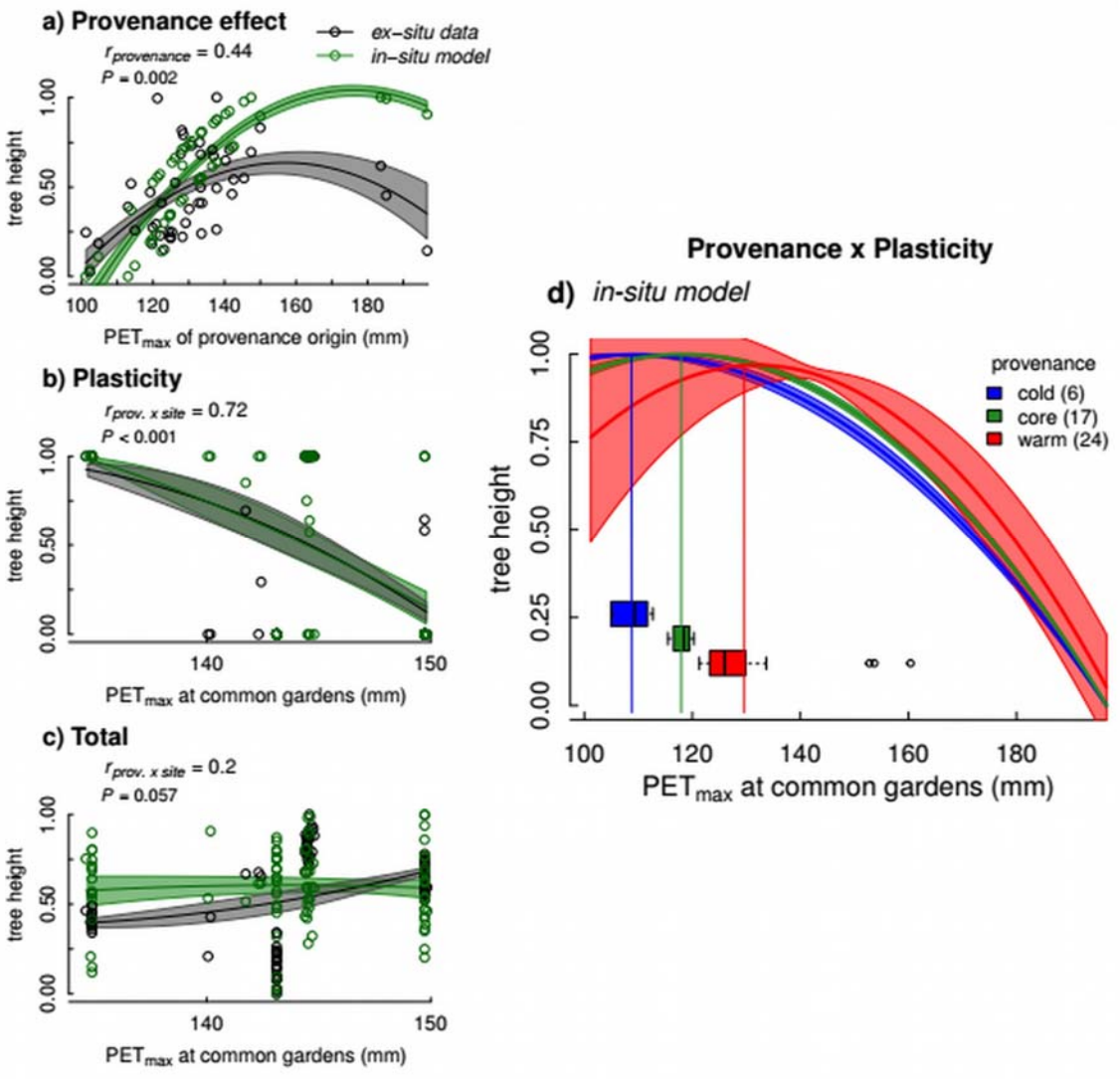

548

549 **Figure 3**

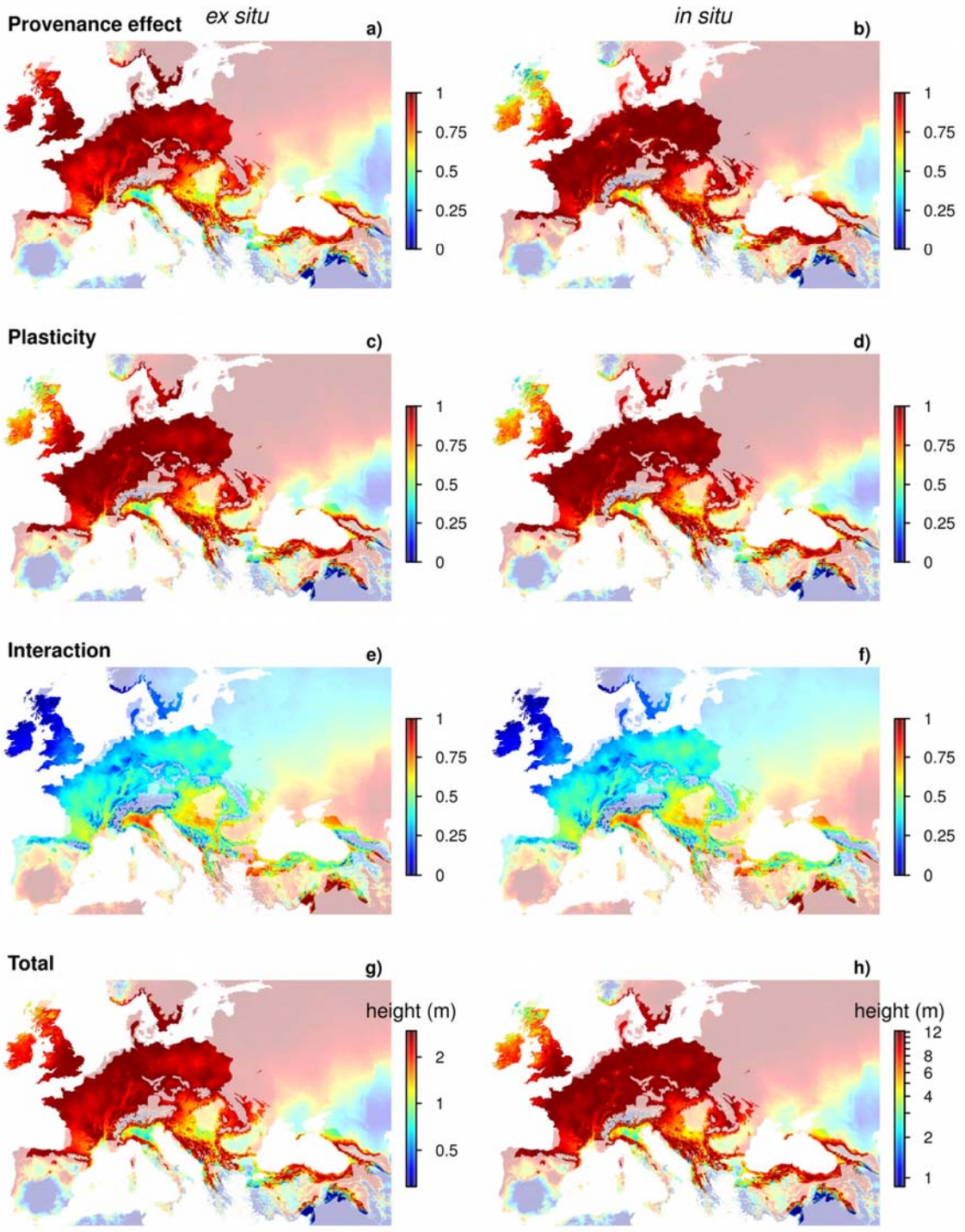

Figure 4

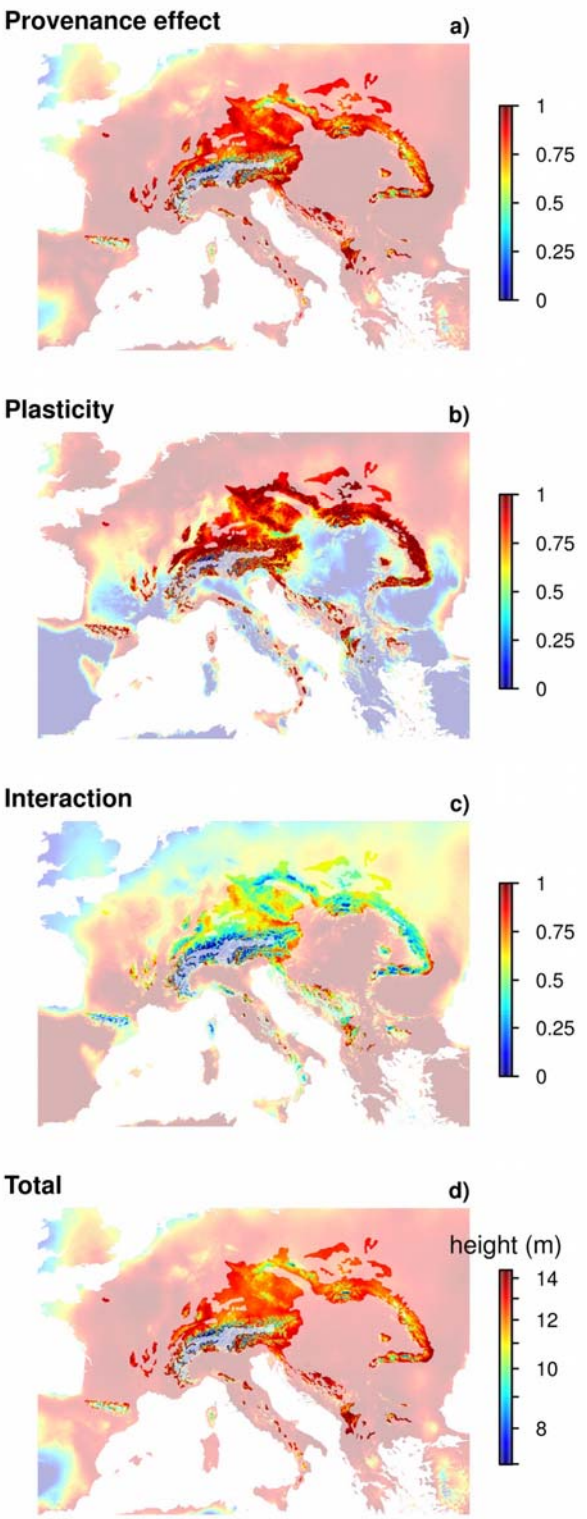

552

553 **Figure 5**